International Journal on
"Technical and Physical Problems of Engineering"
(IJTPE)
Published by International Organization of IOTPE

ISSN 2077-3528
IJTPE Journal
www.iotpe.com
ijtpe@iotpe.com

December 2020 | Issue 45 | Volume 12 | Number 4 | Pages 103-108

PV BASED *V/F* CONTROLLED INDUCTION MOTOR DRIVE FOR WATER PUMPING

N. Genc

Department of Electrical-Electronics Engineering, Yalova University, Yalova, Turkey, naci.genc@yalova.edu.tr

Abstract- Induction motor applications need a DC source include DC-DC power electronics circuits that can generate DC bus voltage before inverter which is needed to implement *V/f* control for speed control in a wide range. In this study, *V/f* speed control has been performed by modeling a three-phase asynchronous motor (induction motor) fed from solar photovoltaic (PV) system. The proposed PV based induction motor (IM) drive for water pumping is composed of two stages of power conversion. While the first stage is to obtain the maximum power from the solar PV array through the interleaved DC-DC boost circuit using the Perturb and Observation (P&O) maximum power point tracking (MPPT) technique, the second stage is the controlling of three-phase induction motor which fed a water pumping by using *V/f* speed controller. The proposed PV based *V/f* controlled IM driver for the water pumping system was designed and its model was simulated in MATLAB/Simulink simulation program. The results of the whole system model were evaluated via Matlab simulation program.

Keywords: PV, MPPT, Induction Motor, Water Pumping.

1. INTRODUCTION

The need for electricity is increasing in the recent times due to the rapid growth of industry and population, at the same time the price of electricity is constantly increased. To satisfy the energy demands and reduce the electricity price renewable energy resources such as solar energy is used, and it is a suitable way to reduce environmental pollution and the using of fossil for energy [1-2]. The generation of electric energy from solar energy via PV panel is widespread because it is easy and simple for implementations, clean, free, maintenance, used for both connected to grid (on-grid) and not connected to grid (off-grid) systems [3]. To overcome the low energy conversion efficiency disadvantage of PV panels, the MPPT method is used, which enables us to extract the maximum generated power from solar panels.

MPPT methods are essentially electronic components with control content used to obtain maximum power from PV modules in any metrological term value (radiation, temperature) by using DC-DC power converters. [4-7]. Boost type DC-DC converters are the most popular among these topologies. The main advantages of the boost converter are simple control reliability. Interleaving of two or more converters has been proposed to increase the rated power value and reduce the current ripple in DC-DC converters [8-9]. This technique consists of proportional phase shift of the control signals of several cells operating in parallel at the same switching frequency. If this technique is used, the input current ripple amplitude is reduced in DC-DC step-up converter.

Motor pump systems used for water supply in rural areas often have high maintenance costs and create pollution. Therefore, in rural areas where there is no grid connection, water pumping systems fed by an external source independent of the grid are used. PV systems are an important resource for motor pump systems in such places. Both DC and AC motors can be used in solar based pumping systems. Since DC motors require maintenance frequently, AC type motors are generally used in these type applications.

Induction motors (IMs) provide desired performances for many industrial applications since they are economical and efficient [10]. IM drives used in solar PV pumping systems include an MPPT circuit with a DC-DC converter to obtain maximum power and a suitable voltage source inverter (VSI) to get maximum efficiency from the motor. The input DC bus voltage regulation of the inverter is provided by VSI itself. In addition, vector controller is generally used in these systems by applying to DC-AC inverter to improving the efficiency of three-phase IMs.

In this study, the *V/f* speed controlled a three-phase IM fed from a solar PV system for water pumping is evaluated. The proposed solar PV water pumping system includes two stages of power conversion. While the first stage is to obtain the maximum power from the solar PV array through the interleaved DC-DC boost circuit using the Perturb and Observation (P&O) maximum power point tracking (MPPT) technique, the second stage is the controlling of three-phase induction motor which fed a water pumping by using *V/f* speed controller. The proposed PV based *V/f* controlled IM driver for the water pumping system was designed and its model was simulated in MATLAB/Simulink simulation program. The results of the whole system model were evaluated via Matlab simulation program.

2. SYSTEM DESCRIPTION

The solar PV based *V/f* controlled IM-water pump driver is shown in Figure 1. The proposed system includes two stages of power conversion. The first stage includes P&O-MPPT technique based PV system to obtain the maximum power from the PV panels. P&O method which is the widespread MPPT algorithm particularly for low priced implementation is applied via an interleaved DC-DC boost converter to get the maximum power from the solar PV array. The interleaved boost DC-DC converter includes two boost stages for increasing the rated power value and reduce the current ripple in DC-DC converter.

The two switches of the interleaved boost DC-DC converter has phase shifted of the control signals at the same switching frequency. By this technique, the ripple amplitude of the input current is reduced via phase-shifted interleaved boost DC-DC converter. The controlling of three-phase induction motor which fed a water pumping by using *V/f* speed controller is the second stage of the system. The three-phase inverter, which is the basis of the three-phase IM drive, consists of six switches (S_1, S_2, S_3, S_4, S_5 and S_6) and provides the three-phase AC voltage required for IM. For IM speed control, the switch trigger of the three-phase inverter is generated using the *V/f* control method.

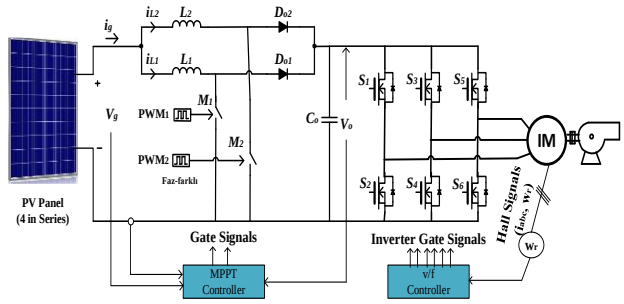

Figure 1. The solar PV based IM driver circuit for water pumping

2.1. Model of the PV Panel

The mathematical model of the PV panel which is selected as YGE Solar YL250P-29b PV module is obtained by selecting as a single-diode model (Figure 2 shows the equivalent circuit of the single diode cell model). Table 1 shows the electrical characteristics of the YGE Solar YL250P-29b PV panel.

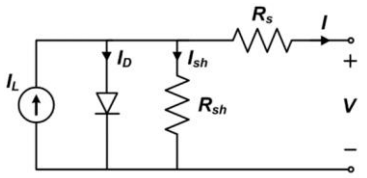

Figure 2. The single diode PV cell model

where, $I_L = I_{ph}$ is the photocurrent; I_D is the diode parallel current; I_{sh} is the shunt current; I is the cell output current; V is the cell output voltage; R_{sh} is the shunt resistance and R_s is the series resistance of the cell model.

Table 1. Parameters of YGE Solar YL250P-29b

Electrical Characteristics	YL250P-29b PV Panel
Max output power (P_{max})	250 W
Max output power tolerances (ΔP_{max})	-5 / + 5 W
PV panel efficiency (η_m)	15.3 %
Voltage at maximum power (V_{mpp})	29.8 V
Open-circuit voltage (V_{oc})	37.6 V
Current at maximum power (I_{mpp})	8.39 A
Short-circuit current	8.92 A

Using the equations given below, the output current, saturation current, reverse saturation current and photon current of the PV module used in the proposed system can be calculated [11]:

$$I = I_{ph} - I_s \left[e^{\left(\frac{V+I.R_s}{A.N_s V_T}\right)} - 1 \right] - \frac{V + I.R_s}{R_{sh}} \quad (1)$$

$$I_s = I_{rs} \left(\frac{T_{op}}{T_{ref}}\right)^3 \left[e^{\left(\frac{-q\varepsilon_G}{A.k}\left(\frac{1}{T_{op}} - \frac{1}{T_{ref}}\right)\right)} \right] \quad (2)$$

$$I_{rs} = \frac{I_{sc}}{\left[e^{\left(\frac{V_{oc}}{A.N_s V_T}\right)} - 1 \right]} \quad (3)$$

$$I_{ph} = (G/1000) \cdot (I_{sc} + \alpha_{I_{sc}} \cdot \Delta T) \quad (4)$$

where, G is irradiance (W/m^2), $\Delta T = T_c - T_{c,ref}$ (operating cell temperature-cell temperature), I_{sc} is short circuit current (A) at STC, α_{Isc} is temperature coefficient and I_{rs} is reverse saturation current of the diode

In order to obtain the correct mathematical equations of a PV module or PV panel used in the applications, the R_P and R_S resistance values must be accurately estimated. Reliable mathematical equations are obtained from the PV module circuit created with reliable R_P and R_S resistance values. Using Equations (1)-(4), the electrical properties and equivalencies of the PV module are applied to MATLAB / Simulink subsystems. The outputs produced from the PV panel module are verified according to the electrical characteristics of the YGE Solar YL250P-29b PV panel. Figure 3 shows the *P-V* curing of the applied PV module with its corresponding MPP under constant temperature.

2.2. Interleaved Boost Topology and MPPT

The power capacity of the conventional single switch boost DC-DC converters is limited for some reasons. These reasons; as the current is increased, the current stresses on the switching elements increase, the reverse conversion currents of the diodes and the resonant currents formed are high enough to exceed the nominal limits of the elements. By increasing the current, the size of the inductor used should be increased in order to avoid high heating and saturation problems. Because of these limitations, the paralleling methods described below have been developed to increase the power capacity of the conventional single-switch boost circuit.

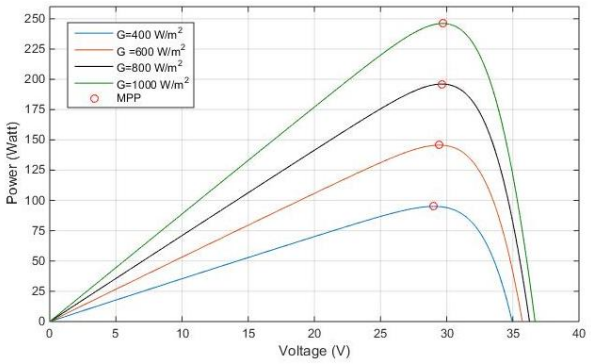

Figure 3. *P-V* curve of the PV (for constant temperature of 25 ºC)

As can be seen in Figure 4, paralleling the power stages by triggering the switches via phase-shifted provides the advantages of classical converter paralleling and also reduces the ripple ratio of the input current. The input current of the circuit is equal to the total summation of the current drawn by the power stages connected in parallel. Since all switches are switched with phase-shifted signals, while the current of any one or more power stages increases, the currents of the other power stage or power stages decrease. Therefore, the ripple ratio of the input current, which is the total summation of the currents of the power stages, decreases.

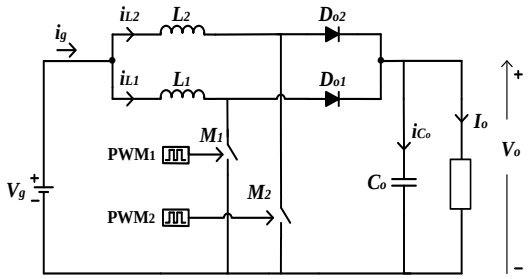

Figure 4. The interleaved boost circuit

The steady state analysis of the interleaved boost DC-DC circuit given in Figure 5 was performed for a two-channel circuit with CCM inductor current waveform. The operating states of the two-channel interleaved boost circuit is related to duty cycle (d). The operating states of the two-channel interleaved boost circuit for d<0.5 are given in Figure 5 [12]. The steady-stated equation of the interleaved topology is also given in Equation (5).

$$X_{kd} = -A^{-1}BU = \begin{bmatrix} i_{L1} \\ i_{L2} \\ V_o \end{bmatrix} = \begin{bmatrix} \dfrac{V_g}{2R_o(1-d)^2} \\ \dfrac{V_g}{2R_o(1-d)^2} \\ \dfrac{2R_oV_g(1-d)}{2R_o(1-d)^2} \end{bmatrix} \quad (5)$$

The main purpose of MPPT controllers is to monitor the maximum power of PV systems. The output power of PV systems varies with variables such as temperature and solar radiation. Therefore, it is necessary to dynamically adjust the operating point of PV systems so that the output power depends on variables such as solar radiation and temperature. This can be done with the MPPT technique. MPPT implementation can be realized with a DC-DC power electronics topology placed after the PV source to manage the commands sending by the tracking algorithm.

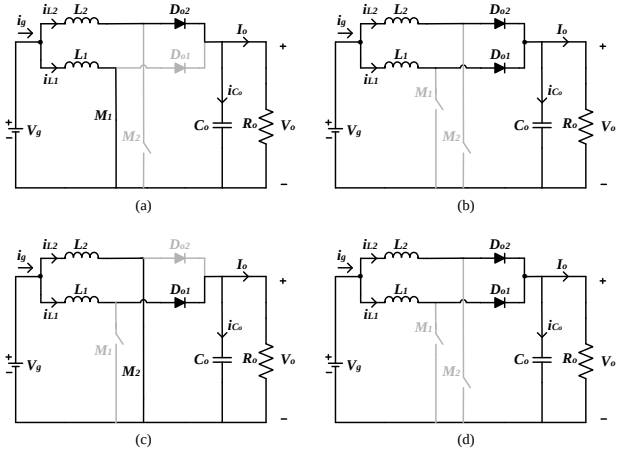

Figure 5. The operating states of the two-channel interleaved boost circuit for d<0.5

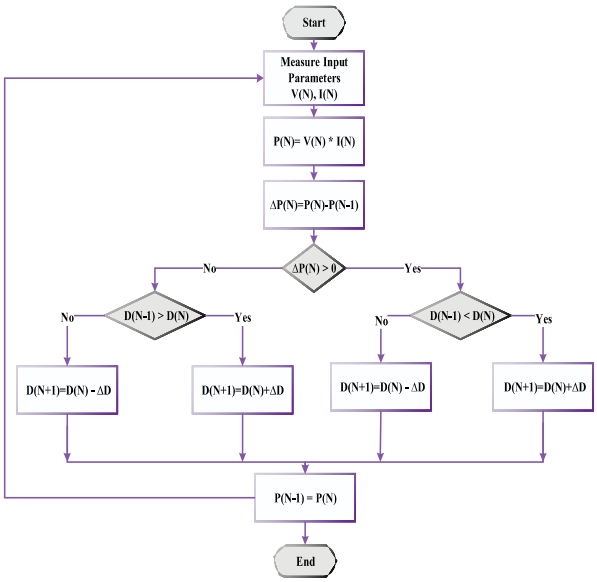

Figure 6. P&O method flowchart

The P&O method, whose flow diagram is given in Figure 6 and is the simplest method of the MPPT technique, operates on the basis of the power change expressed in Equation (6). P&O method operates in the direction where the power obtained from the PV system increases.

$$\Delta P = P(N) - P(N-1) \quad (6)$$

As can be understood from the flow diagram of the P&O MPPT method and the equation quoted above, if the change of output power obtained from the PV system is positive, the change in duty factor (D) applied to the DC-DC converter will increase towards the increase in power so as to provide voltage change. If the change of output power obtained from the PV system is negative, the change in duty factor (D) applied to the DC-DC converter will change towards the decrease in power.

2.3. IM Model and *V/f* Control Method

The IM equivalent circuit is a subject frequently quoted in the literature. The equivalent circuit of an IM with the rotor windings shorted or the equivalent circuit of a squirrel-cage IM is the same as a transformer model with shorted secondary windings. The coupling coefficients between the stator and rotor phases of the induction motor vary according to the rotor rotation angle. The mathematical model of the induction motor can be obtained as a set of differential equations using mutual inductances. The mathematical model equations obtained using the d, q reference frame of the three phase IM and the expression for the electromagnetic torque are as follows.

$$T_e = \frac{3}{2}.\frac{p}{2}.\frac{1}{\omega_b}.(F_{ds}i_{qs} - F_{qs}i_{ds}) \quad (7)$$

$$T_e - T_L = \frac{2}{p}.J.(\frac{d\omega_r}{dt}) \quad (8)$$

$$v_{dq0}^{s} = \frac{2}{3}\begin{bmatrix} 1 & -1/2 & -1/2 \\ 0 & -\sqrt{3}/2 & \sqrt{3}/2 \\ 1/2 & 1/2 & 1/2 \end{bmatrix} \quad (9)$$

where, T_e and T_L are the electromagnetic and load torque, respectively, J is the constant inertia value of the IM and ω_r is the rotor speed of the machine.

V/f controller is the most widely used asynchronous motor driving method in the industry. Its price is more affordable due to its ease of application. In *V/f* constant ratio control, the voltage starts from a value called "boost" and gradually climbs up to the motor operating voltage. In this case, the frequency also climbs with the voltage. For example, if a 400 V, 50 Hz asynchronous motor is driven, the frequency gradually increases from 20 Volt input to the end of 400-volt climb. The slope of this climb gives the ratio *V/f*, and the frequency climbs between 0-50 Hz until the motor reaches full capacity. When the voltage reaches 400 V, the speed of the IM can be controlled easily by changing the frequency.

With this method, speed control of asynchronous motors is easily realized. It is possible to start the motor at nominal torque even with the stator at rest, and not to draw high currents from the line. The main reasons of speed control with this method are that large and high inertia loads are desired to be loaded on the rotor at the start of the motor.

Synchronous speed (stator magnetic field speed) can be adjusted by changing the applied stator frequency, and according to synchronous speed the rotor speed can be adjusted. As the frequency is increased, the speed increases, and when it is decreased, the speed decreases. However, this setting has a limitation. The smaller the frequency, the smaller the equivalent circuit impedance. If the applied voltage is kept constant during this time, the current will also increase. In this case, large current values occurring in the stator due to the excessive current drawn cause the machine to be magnetically saturated. This may cause the winding to burn.

In order to keep the magnetic flux value constant, in regions below the nominal frequency of asynchronous motors, the voltage applied to the stator is changed in the same proportion in addition to the frequency. So, *V/f* ratio is kept constant. This form of speed control is sometimes called scalar control. In the region after the nominal frequency, the residual voltage value is kept constant at the nominal level and only the frequency is changed.

An inverter is connected to the grid or DC source just before the motor to adjust the *V/f* ratio. Pulse width modulation (PWM) technique is generally used in the inverter to bring the voltage to the desired frequency and amplitude level. In other words, DC voltage supplied via DC source or converter is converted to AC voltage with the help of a DC-AC inverter with frequency and amplitude adjusted. The main point to note here is that although *V/f* is a constant ratio, the ratio of the derivatives of voltage and frequency with respect to time is also fixed, but the rate of change over time has no binding effect. The rate of change in the time to be adjusted can be fixed according to the motor power.

While full frequency is reached in a shorter time in small rotor motors, it takes longer time to reach full frequency in large rotor motors. The main reason for this is that the frequency change will increase the magnetic flux without reaching the speed of the rotor in the frequency value, causing the current to increase and to shift. This increases the power loss in large engines. Figure 7 shows the *V/f* fixed rate control block diagram.

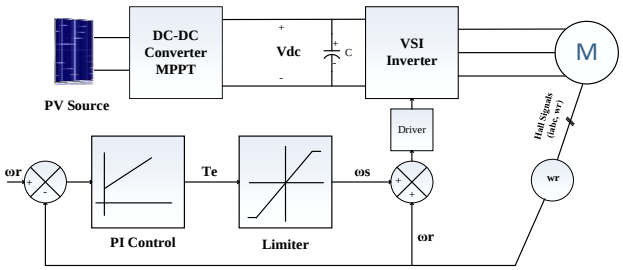

Figure 7. The *V/f* fixed rate control block diagram for IM

3. RESULTS AND DISCUSSION

The proposed study has been verified via some simulation results which were obtained via Matlab/Simulink program. Table 2 gives components and parameters of the IM used in simulations.

Table 2. Parameters of the IM

Components	Symbols	Parameters
IM rated power	P_m	1 kW
IM stator resistance	R_s	0.82 Ω
IM stator inductance	L_s	0.005 H
IM rotor eqv. resistance	R_r	0.95 Ω
IM rotor eqv. inductance	L_s	0.17 H
IM inertia	J	0.007 kg.m^2
IM pole number	p	4

First, the verification of MPPT controller is explained. Verification of the system is important to produce an effective knowledge of proposed MPPT system in application study. The PV system has been simulated under constant irradiance and temperature, then the variations in the inputs have been evaluated. To verify the P&O method, a uniform radiance and temperature are

chosen to verify whether it is producing the optimal duty cycle to the interleaved boost converter or not. For this case, the irradiance and temperature are constant at 1000 W/m^2 and 25 ^{o}C. Using P&O controller, the generated power, current and voltage of PV panels is showing in Figure 8, it clearly shows that the PV panels is operating at MPPT. The voltage and current of the PV system are 4×29.8 V and 8.1 A which present the power of the MPPT (about 1000 W).

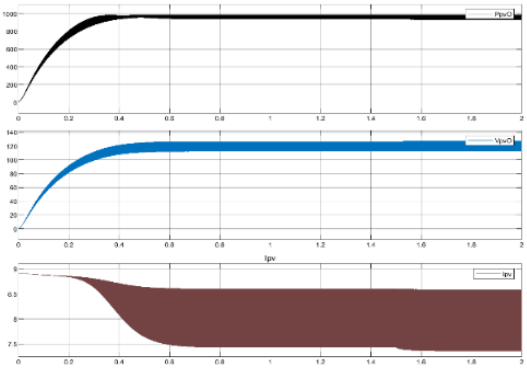

Figure 8. Simulation results of PV system with MPPT under constant irradiance and temperature (power, current and voltage of PV panels)

The generated output power, output current and output voltage of the interleaved DC-DC boost converter is showing in Figure 9, it clearly shows that the PV panels transfer the maximum power to the load (about 1000 W). Since the proposed PV system includes 4×250 W PV panels in series, the voltage of the system is increased while the current of the PV system is equal to one PV panel. The generated output power of the interleaved DC-DC boost converter is increased by increasing this voltage via MPPT.

The simulations have been also applied to P&O MPPT controller based PV system to compare the power values of the PV system and output power under constant and variable irradiance values. While Figure 10 shows the power results of PV system and interleaved boost converter with MPPT under constant irradiance, Figure 11 shows the power results of PV system and interleaved boost converter with MPPT under variable irradiance. It is seen that the MPPT controller provide maximum power from PV system under both conditions.

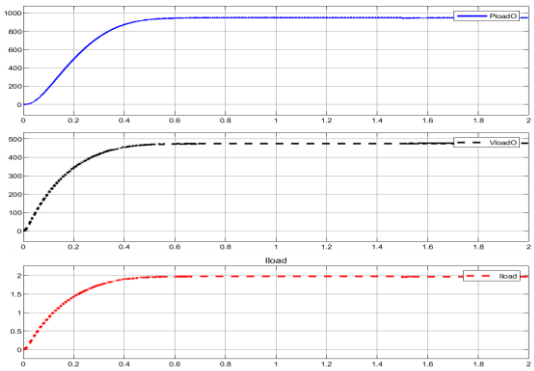

Figure 9. Simulation results the interleaved DC-DC boost converter with MPPT under constant irradiance and temperature

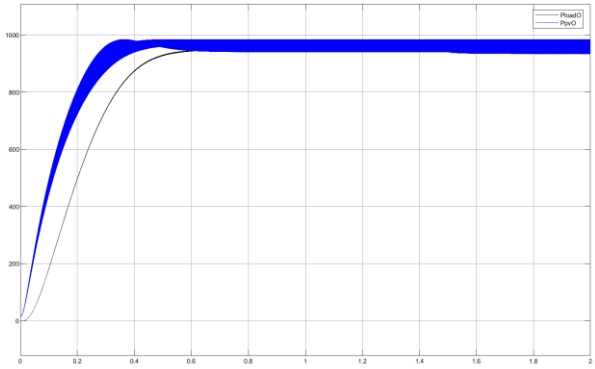

Figure 10. Simulation power results of PV system and interleaved boost converter with MPPT under constant irradiance and temperature

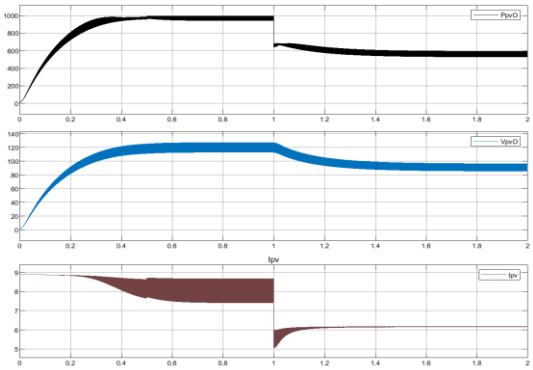

Figure 11. Simulation results of PV system with MPPT under variable irradiance (power, current and voltage of PV panels)

Speed control of the IM was realized by applying *V/f* control to the induction motor fed by the P&O MPPT controller based PV-Interleaved boost system. The IM was controlled at 1500 rpm under 5 Nm load and then the dynamic response of the controller was observed by reducing the reference speed to 1000 rpm.

As can be seen in Figure 12, the rotor speed has stabilized following the given speed trend with a delay of 0.15 seconds at the start of the motor. When it reaches 1500 rpm, it was able to follow almost exactly the same speed trend. Like the rise of the cycle, its fall is included in the trend of speed. At t=2, the engine speed was reduced from 1500 rpm to 1000 rpm. The response of the system was in the form of damped oscillation. The region where the damping oscillation is greatest is about 6% of the total motor speed and has decreased to less than 0.5%. Once stabilized, the motor rotation speed became almost the same as the desired rotation speed.

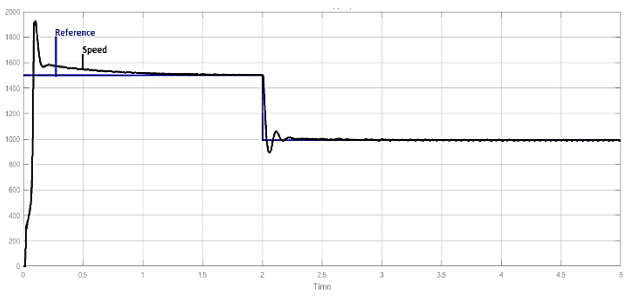

Figure 12. Rotor speed of *V/f* controlled IM under 5 Nm load.

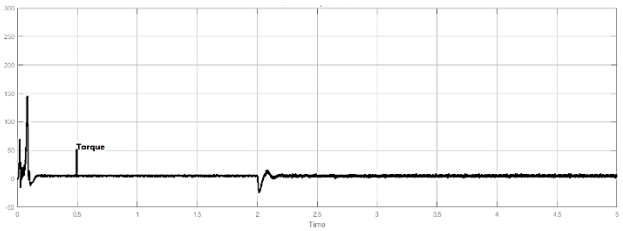

Figure 13. Electromagnetic torque of *V/f* controlled IM under 5 Nm

The electromagnetic torque graph shown in Figure 13 oscillates positive in the parts where the speed increases, negative in the parts where it decreases, and around 0 in the parts where it is stable in accordance with the speed trend. While the load has a negative effect in the parts where the speed increases, it has a positive effect in the parts where it decreases, causing the electromagnetic torque to increase in the speed increase and the electromagnetic torque to decrease in the speed decrease.

4. CONCLUSIONS

This study presents simulation results related to the *V/f* speed controlled a three phase IM fed from a solar PV source for water pumping. The results of the whole system model were evaluated via Matlab simulation program. An interleaved DC-DC boost converter is used to extract maximum power from the solar PV system. It has been observed that the P&O MPPT controller based interleaved DC-DC boost converter reduces the current ripple drawn from the PV system and provides maximum power. The power results of PV system and interleaved boost converter with MPPT under constant and variable irradiance are evaluated and compared. It is seen that the MPPT controller provide maximum power from PV system under both conditions. The IM motor speed control (*V/f*) has been observed at 1500 rpm under 5 Nm load and then the dynamic response of the controller was observed by reducing the reference speed to 1000 rpm. While examining the dynamic effect of the *V/f* controller applied for IM, the dynamic response of the P&O MPPT controller based interleaved DC-DC converter has been investigated. It will better to verify the proposed topology with experimental results. Experimental study can be considered as a future work.

REFERENCES

[1] I. Kocaarslan, S. Kart, Y. Altun, N. Genc "Lyapunov Based PI Controller for PEM Fuel Cell Based Boost Converter", International Journal of Renewable Energy Research-IJRER, Vol. 10, No. 1, pp. 275-280, 2020.

[2] H.A. Shayanfar, G. Derakhshan, A. Ameli, "Optimal Operation of Microgrids Using Renewable Energy Resources", International Journal on Technical and Physical Problems of Engineering (IJTPE), Issue 10, Vol. 4, No. 1, pp. 97-102, March 2012.

[3] A. Karafil, H. Ozbay, S. Oncu, "Design and Analysis of Single-Phase Grid-Tied Inverter with PDM MPPT-Controlled Converter", IEEE Transactions on Power Electronics, Vol. 35, No. 5, pp. 4756-4766, May 2020.

[4] E. Irmak, N. Guler, "Application of a High Efficient Voltage Regulation System with MPPT Algorithm", International Journal of Electrical Power & Energy Systems, Vol. 44, No. 1, pp. 703-712, 2013.

[5] A. Karafil, H. Ozbay, M. Kesler, "Temperature and Solar Radiation Effects on Photovoltaic Panel Power", Journal of New Results in Science, Vol. 5, No. 12, pp. 48-58, 2016.

[6] J.A. R. Hernanz, J.M. L. Guede, et al., "Analysis of the Algorithm P&O for MPPT", International Journal on Technical and Physical Problems of Engineering (IJTPE), Issue 31, Vol. 9, No. 2, pp. 6-14, June 2017.

[7] H.C. Lu, T.L. Shih, "Design of DC/DC Boost Converter with FNN Solar Cell Maximum Power Point Tracking Controller", IEEE Conference on Industrial Electronics and Applications, 2010.

[8] N. Genc, Y. Koc, "Experimental Verification of an Improved Soft Switching Cascade Boost Converter", Electric Power Systems Research, 149, pp. 1-9, 2017.

[9] H.M. Farh, M.F. Othman, et al., "Maximum Power Extraction from a Partially Shaded PV System Using an Interleaved Boost Converter", Energies, Vol. 11, No. 10, pp. 2543, 2018.

[10] K. Kim, A.G. Parlos, A.G. Bharadwaj, "Sensorless Fault Diagnosis of Induction Motors", IEEE Trans. Ind Electron., Vol. 50, No. 5, pp. 1038-1051, 2003.

[11] D. Haji, N. Genc, "Dynamic Behaviour Analysis of ANFIS Based MPPT Controller for Standalone Photovoltaic Systems", International Journal of Renewable Energy Research-IJRER, Vol. 9, No. 1, pp. 101-108, 2020.

[12] N. Genc, I. Iskender, "Steady State Analysis of a Novel ZVT Interleaved Boost Converter", International Journal of Circuit Theory and Applications, Vol. 39, pp. 1007-1021, 2011.

BIOGRAPHY

Naci Genc received his B.Sc., M.Sc., and Ph.D. degrees from Gazi University (Ankara, Turkey), Van Yuzuncu Yil University (Van, Turkey) and Gazi University in 1999, 2002, and 2010, respectively. He is a Professor in the Electrical-Electronics Engineering Department of Yalova University (Yalova, Turkey). His interests include energy conversion systems, power electronics and electrical machines.